Sensors and Actuators B 240 (2017) 186–192

Contents lists available at ScienceDirect

Sensors and Actuators B: Chemical

journal homepage: www.elsevier.com/locate/snb

Thermal stability of the sensing properties in H_2 sensors composed of Pd nanogaps on an Elastomeric Substrate

Byungjin Jang[a,1], Wonkung Kim[a,1], Min-Jung Song[b,*], Wooyoung Lee[a,*]

[a] Department of Materials Science and Engineering, Yonsei University, 262 Seongsanno, Seoul 120-749, Republic of Korea
[b] College of Liberal Art & Interdisciplinary Studies, Kyonggi University, 154-42 Gwanggyosan-ro, Yeongtong-gu, Suwon-si, Gyeonggi-do 443-760, Republic of Korea

ARTICLE INFO

Article history:
Received 27 June 2016
Received in revised form 9 August 2016
Accepted 24 August 2016
Available online 25 August 2016

Keywords:
Palladium (Pd)
Nanogap
Hydrogen sensors
Poly(dimethylsiloxane) (PDMS)
Thermal stability

ABSTRACT

The influence of thermal exposure on sensing properties of H_2 sensor based on Pd MOTIFE (highly mobile palladium thin films on an elastomer) was investigated. This sensor was fabricated on a Poly(dimethylsiloxane) (PDMS) substrate and its Pd nanogaps were obtained through mechanical stretching and H_2 exposure. When the substrates were annealed at 80–200 °C, wrinkles were formed to release the stress due to the mismatch of the thermal expansion coefficients between the PDMS layer and the Pd film. The wrinkling wavelength and the compressive stress of the Pd/PDMS layers were estimated using simple equations as a function of the annealing temperature. The width of the Pd nanogaps of the annealed samples was measured using SEM analysis. Higher annealing temperatures led to a decrease in the wrinkling wavelength and an increase in the width of the Pd nanogap. This was attributed to increases in the individual variation of the compressive stress and strain between PDMS and the Pd/PDMS layers. The enlarged Pd nanogap contributed to a decrease in the performance of the sensor. Nevertheless, the Pd sensor exhibited perfectly on-off operation with a response time of less than 1 s when annealed at temperatures up to 100 °C.

1. Introduction

Hydrogen (H_2), a colorless, odorless, and tasteless gas, has attracted significant attention as a clean alternative energy source [1]. It occupies 75% of the mass of the universe and produces only water and no harmful by-products by combustion [2]. However, hydrogen involves high risks such as high flammability (4–75.6% in oxygen/air), large diffusion coefficient (0.61 cm^2/s), low ignition energy (0.02 mJ) and large flame propagation velocity [3]. Therefore, rapid and accurate H_2 detection is of practical importance in various fields. As a result, the development of accurate H_2 sensors is essential to secure its safety [4]. To date, H_2 gas sensors have been mainly developed using various materials including metals [5], semiconductor oxides [6], nanocarbons [7], and conducting polymers. [8] Among them, palladium (Pd) has been extensively applied due to its unique ability to absorb/desorb molecular H_2 [9–13]. On exposure to H_2, Pd is converted to the Pd-H hydride through H_2 absorption, accompanied by α-β phase transition [14,15]. It causes the expansion of its volume to up to 900 times, resulting in the variation of its electrical resistance in accordance with the H_2 concentration [16].

In a previous study, we developed hydrogen sensors composed of Pd-based MOTIFE (highly mobile palladium thin films on an elastomer) [17–21], which was the lithography-free nanogap sensor using reversible swelling of the multiple cracked Pd films. The nanogaps were produced through the crack propagation on an elastomeric substrate. This sensor operates as a perfect on-off mode through to H_2 absorption/desorption by lattice expansion or contraction of Pd layer. Moreover, it exhibits advantages including simplicity of fabrication, low cost, and high performance (e.g., low detection limit and fast response time). However, considering that the elastomeric substrate can undergo thermal deterioration at high temperatures, the stability of these sensors towards temperature is required to assess the possibility of commercial applications.

In this study, we have demonstrated the influence of thermal exposure of the Pd based MOTIFE H_2 sensor for the first time by annealing at temperatures up to 200 °C. The Pd based MOTIFE sensors were fabricated using a simple mechanical stretching process and then annealed at 70–200 °C after identifying the on-off response at room temperature. The H_2 sensing performance of the

* Corresponding authors.
E-mail addresses: wooyoung@yonsei.ac.kr (W. Lee), mjsong@kyonggi.ac.kr (M.-J. Song).
[1] These authors contributed equally to this work.

http://dx.doi.org/10.1016/j.snb.2016.08.140
0925-4005/

annealed samples was tested and their Pd nanogap widths were measured as a function of the annealing temperature. Moreover, their buckling wavelengths and the stress at various temperatures were also estimated using simple equations. Based on these results, we suggest the mechanism of formation of enlarged Pd nanogaps with increase in annealing temperature.

2. Experimental details

2.1. Preparation of the Pd MOTIFE H_2 sensors

The MOTIFE nanogap was fabricated by a previously published method [17]. In brief; a PDMS elastomeric substrate (20 mm × 10 mm × 0.75 mm) was prepared. The PDMS monomer (Sylgard 184, Dow Corning Corp.) was mixed with a curing agent in the weight ratio 10:1 and then cured at 75 °C for 4 h on a hot plate. A 10 nm thin Pd layer was deposited on the PDMS substrate by ultrahigh vacuum (UHV) DC magnetron sputtering under 34 sccm of Ar flow. To form the nanogaps on the Pd layer, the specimen was mechanically stretched to up to 50% elongation using stretching equipment built in-house. To study the effect of the annealing temperature on the Pd nanogap, the stretched samples were heat treated for 1 h at various temperatures using a hot plate. Their sensing properties were measured after keeping for 6 h at room temperature.

2.2. Characterization

The surface morphology of the MOTIFE nanogap sensor was observed using field-emission scanning electron microscopy (FE-SEM; JSM-6701F, JEOL Ltd. Japan) and atomic force microscopy (AFM; JPK Inst., Nanowizard I). Phase analysis of the sensor was carried out using High Resolution X-ray diffractometer (HR-XRD; SmartLab, Rigaku). The electrical measurements of the H_2 sensing properties were carried out using a Keithley 236 current source measurement unit (Keithley Instruments, Inc., Ohio, USA) and a gas sensing system consisting of a furnace (Korea Vacuum Tech., Korea; 250 mL), a mass flow controller (MFC), and gas cylinders of the target gas (H_2) and base gas (N_2). The samples were placed in the furnace using a printed circuit board (PCB). N_2 gas was used for venting the chamber. All experiments were repeatedly performed using four samples at room temperature.

3. Results and discussion

Fig. 1 shows the schematic of the fabrication of the Pd-based MOTIFE sensors and the SEM images of the sample surface morphology corresponding to each step. The deposited Pd thin films exhibited very uniform and smooth surfaces (Fig. 1a). Vertically aligned nanocracks were initiated on the surface of the Pd films deposited because of the mechanical stretching, which appeared at intervals of about 15 μm. After repeated cycles of exposure to H_2/N_2, the nanocracks were converted to more stable nanogaps (Fig. 1b). These nanogaps resulted from the volume expansion/contraction of Pd by H_2 absorption and desorption, which is a unique behavior of elastomeric substrates [17]. As a result of the heat treatment, the Pd film on the PDMS substrate buckled into sinusoidal waves vertically against the nanogap, as shown in Fig. 1(c). It is well known that PDMS and Pd thin films experience thermal expansion during heat treatment and then shrink to their initial dimensions while undergoing cooling to room temperature, resulting in compressive stresses in the film [22–25]. The wrinkles originate from a mismatch of the thermal expansion coefficients between the Pd film (11.8×10^{-6}/°C) and the PDMS polymer layer (310×10^{-6}/°C). The buckling occurs because of stress release from the surface of the Pd film.

Table 1
The constants of thermal expansion coefficient for palladium metal.

Metal	$a_1 \times 10^{-6}$	$a_2 \times 10^{-9}$	Temperature range, °C
Palladium	12.10	2.000	20–900

The wrinkling wavelength (λ) is theoretically predicted by Eq. (1) [26].

$$\lambda = 4.36t\left(\frac{E_m\left(1-\nu_p^2\right)}{E_p\left(1-\nu_m^2\right)}\right)^{\frac{1}{3}} \approx 4.4t\left(\frac{\bar{E}_m}{\bar{E}_p}\right)^{\frac{1}{3}} \quad (1)$$

The subscripts m and p refer to the metal (Pd) and the polymer (PDMS), t (m) is the thickness of the Pd film, E (GPa) is the Young's modulus (or elastic modulus), $\bar{E} = E/\left(1-\nu^2\right)$ is the plane-strain modulus, and ν (dimensionless) is the Poisson's ratio ($\nu_m = 0.39$ for Pd and $\nu_p = 0.5$ for PDMS). E_m and E_p for Pd and PDMS are obtained by Eq. (2)–(3), respectively [27,29].

$$E_m = 3K_T(1-2\nu) \quad (2)$$

$$E_p = \frac{3}{2}k_B \cdot T \cdot \rho_k \quad (3)$$

Here, K_T is the bulk modulus; k_B is the Boltzmann constant, T is the temperature, and ρ_k is the degree of crosslinking density. In the literature, the elastic modulus for PDMS (Sylgard 184) is 1.75 MPa at room temperature and the degree of crosslinking density is 4.93×10^{26} m^{-3} under the 10:1 condition [28]. The bulk modulus K_T is expressed by Eq. (4) as a function of temperature and this relationships process is explained detail in Supporting information.

$$K_T = K_{T_0}\left(\frac{a_1 + 2a_2T_0}{a_1 + 2a_2T}\right) \quad (4)$$

Where, K_{T0} is 180 GPa for Pd, which is the value of bulk modulus at T_0; a_1 and a_2 are thermal expansion constants, which values for Pd are summarized in Table 1. So, E_m is determined by substituting Eq. (4) in Eq. (2). As a result, the wrinkling wavelength of the Pd/PDMS layer was estimated by substituting Eqs. (2)–(3) in Eq. (1).

For a certain annealing temperature, the parameters including the thermal stress of PDMS (σ_{PDMS}), maximum contraction force (F_{PDMS}), and maximum shear stress at the Pd-PDMS interface ($\sigma_{Pd\text{-}PDMS}$) by the cooling are calculated [28], and their values at various temperatures were listed in Table 2. As shown in Table 2, the elastic modulus of PDMS increases with increase in temperature, and the elasticity is considered as an entropic effect [29]. The values of α and E_m decrease with increase in temperature. In summary, higher annealing temperatures led to a decrease in the wavelength of the wrinkles and λ was theoretically about 1.4–1.6 μm (Table 2). It was supported by the AFM analysis (Fig. 2). From this result, the wrinkle wavelengths showed also a tendency to decrease as annealing temperature increased even though they were not accurately corresponded to the calculated values.

The value of λ determines the critical or minimum strain (ε_c) necessary for the buckling to occur. The critical strain (ε_c) is expressed in Eq. (5) [25].

$$\varepsilon_c = 0.25\left(\frac{3\bar{E}_p}{\bar{E}_m}\right)^{\frac{2}{3}} \quad (5)$$

By substituting Eq. (5) in Eq. (1),

$$\lambda = \pi t\sqrt{\frac{1}{\varepsilon_c}} \quad (6)$$

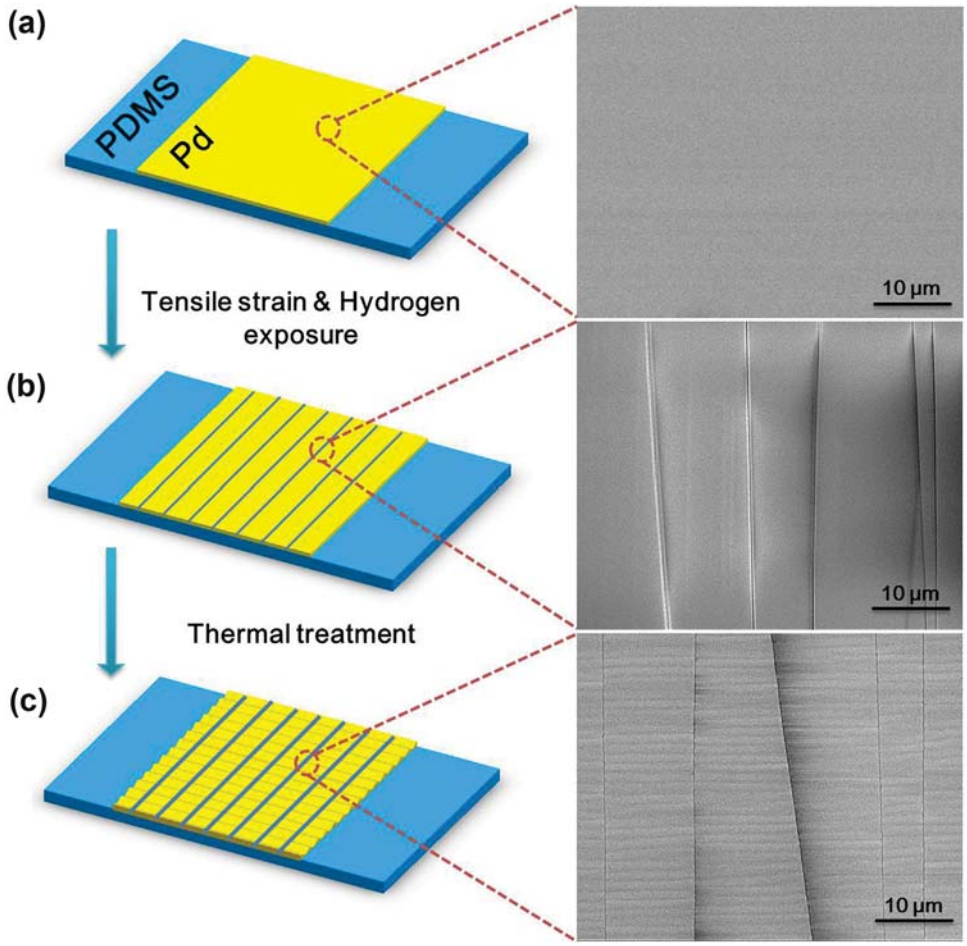

Fig. 1. Schematic representing the fabrication of Pd nanogap sensors on an elastomeric substrate along with the SEM images, respectively. (a) Deposition of the Pd thin film on PDMS and (b) nanogap formation after mechanical stretching and H_2 cycling. (c) Buckling of ordered Pd surface with nanogaps on the PDMS after thermal treatment.

Table 2
The estimated values of the correlation parameters according to annealing temperature.

Temp. (°C)	Palladium			PDMS			Pd/PDMS	
	$\alpha \times 10^{-5}$ (°C^{-1})	K_T (GPa)	E_m (GPa)	E_p (MPa)	σ_{PDMS} (MPa)	F_{PDMS} (N)	λ (μm)	$\sigma_{Pd\text{-}PDMS}$ (kPa)
80	1.245	176.184	116.281	2.108	0.0392	0.2941	1.608	2.941
90	1.250	175.563	115.872	2.167	0.0470	0.3527	1.591	3.527
100	1.254	174.947	115.465	2.227	0.0552	0.4242	1.575	4.142
110	1.258	174.336	115.062	2.287	0.0638	0.4786	1.559	4.786
120	1.263	173.728	114.661	2.346	0.0727	0.5454	1.544	5.454
150	1.276	171.931	113.474	2.526	0.1018	0.7635	1.501	7.635
200	1.298	169.017	111.551	2.824	0.1576	1.1818	1.438	11.818

Hence, λ is inversely proportional to the square root of the critical strain and hence, shorter wavelength originates from higher strain. Moreover, it might affect the size of the Pd nanogap.

To investigate the effect of the annealing temperature on the size of the Pd nanogap, six randomly chosen spots were evaluated on each sample at different temperatures by SEM analysis. The width of the Pd nanogap for each annealing temperature was evaluated by the average value obtained from six spots. As shown in Fig. 3, the width of the Pd nanogap increased linearly with an increase in the annealing temperature, and the mechanism is discussed in detail in Fig. 5.

Fig. 4 shows the H_2 sensing properties of the Pd-based MOTIFE sensors subjected to heat treatment at different temperatures (25–200 °C). The sample at 25 °C was a control sample (Fig. 4(a)). In this sample, the first exposure to 10% H_2 led to the formation of Pd nanogaps through the volumetric swelling/contraction of Pd. Then the on-off response was tested at various H_2 concentrations and the detection limit of the sensor was 0.3%. At annealing temperatures up to 70 °C, the samples exhibited the similar sensing current level with the control sample (data not shown). In case of the sample at 80 °C, the current showed the similar value at high concentrations (more than 1% H_2), but decreased drastically at low concentrations (below 1% H_2). Moreover, the samples annealed at temperatures above 80 °C exhibited lower current levels and higher detection limits in all H_2 concentration range. It might be attributed to thermal denaturalization of elastomer substrate. In other words, the surface buckling on the Pd/PDMS films developed at annealing temperatures more than 80 °C. This result was observed in Fig. 2(c). The sample annealed at 200 °C showed seldom a response in the overall concentration range (Fig. 4(c)). It was regarded that the electric current does not flow because the width of the Pd nanogap is large enough to disconnect the Pd layer. The nanogap width is an

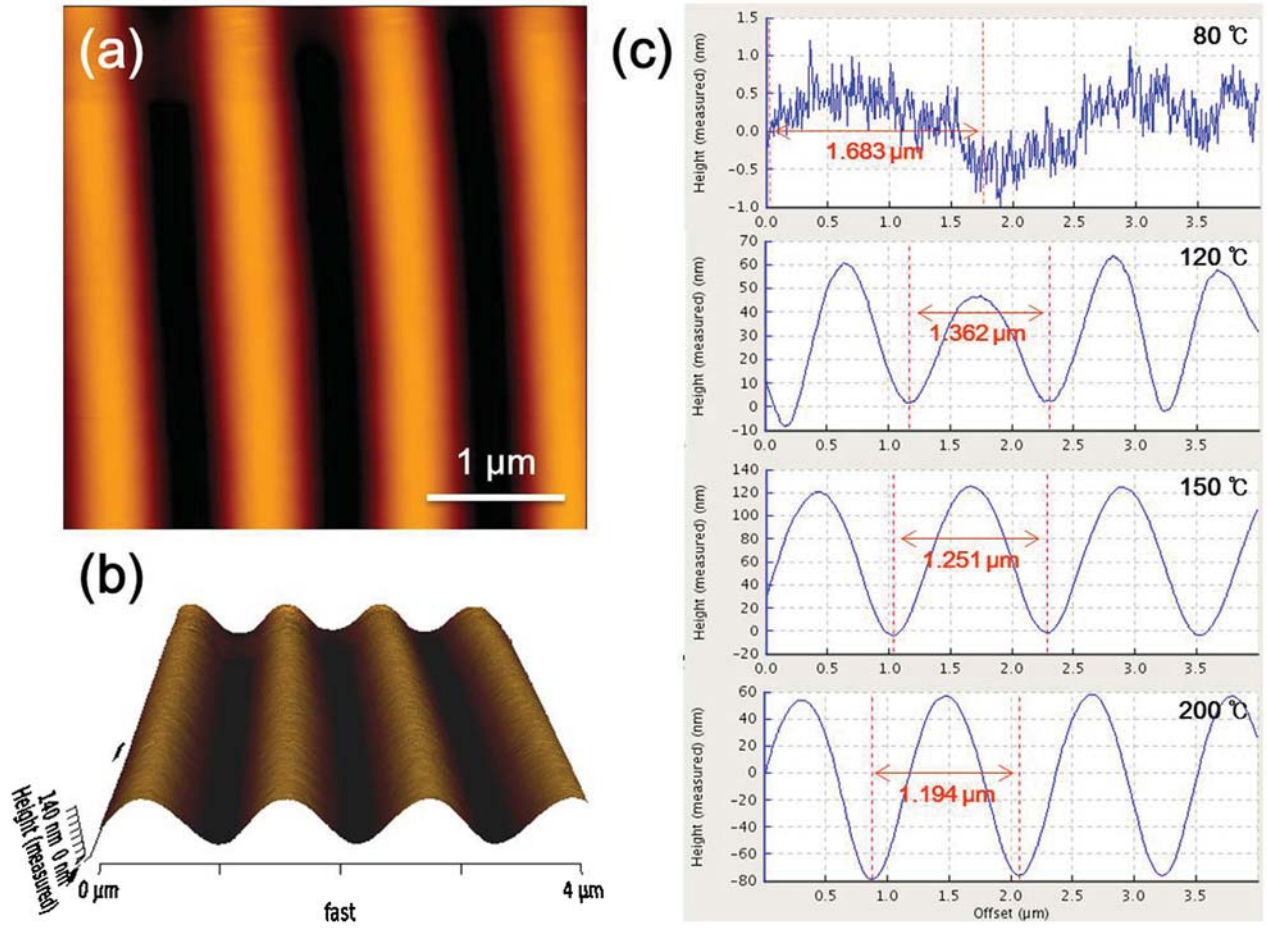

Fig. 2. (a) Surface morphological AFM image of PDMS/Pd sensor annealed at 200 °C and (b) its 3D image. (c) Wrinkle wavelength analysis of Pd nanogap sensor surface with variant annealing temperature condition.

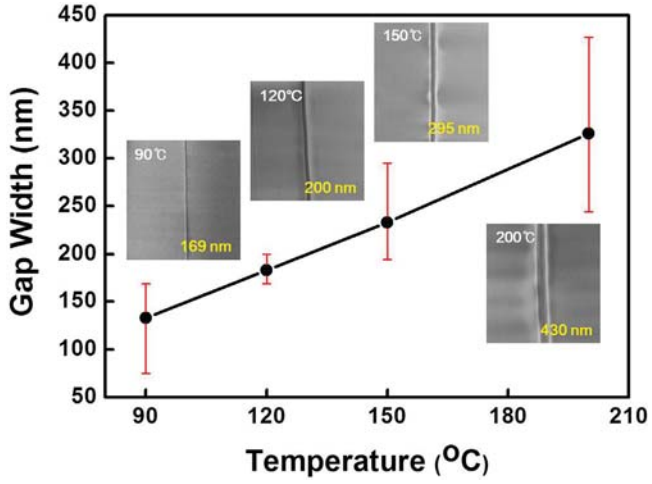

Fig. 3. Temperature dependence of the nanogap length along with the SEM images of the surface of Pd nanogaps. The red line indicates the error. (For interpretation of the references to colour in this figure legend, the reader is referred to the web version of this article.)

important factor in the sensing performance of the Pd-based H_2 sensor [16]. As a result, the smaller width of the Pd nanogap leads to the enhanced sensing performance. The sensor response of the samples annealed at 100 °C is shown in Fig. 4(d). All the samples, except the ones annealed above 150 °C (data not shown), showed this trend. These results indicate a response time of less than 1 s for all concentrations. Generally, the response time is defined as the time to reach 90% of the total change in the electrical resistance at a certain concentration.

Fig. 5 shows the schematic illustration of the formation mechanism of enlarged Pd nanogaps at high annealing temperatures. The enlarged Pd nanogaps might result from increases in the individual variation in the compressive stress and the strain between PDMS and Pd/PDMS layers with increase in the annealing temperature (Table 2). The stress and strain in Pd/PDMS is confirmed by the XRD patterns with different annealing temperature as shown in Fig. 6. The typical Pd peak (111) was observed at pristine Pd/PDMS films (black line), which is not preceding hydrogen uptake. The peak for Pd phase is quite broad because of extremely thin thickness of Pd layer on elastomer substrate. The 2θ values of the Pd peak are gradually shifted to lower values with increase in the annealing temperature, showing the slight increase in the lattice constant of Pd due to relaxation of the stresses from the annealing process. We considered the compressive surface stresses (σ_x and σ_y) in two directions, which as denoted as $\sigma_{x,PDMS}$ and $\sigma_{y,PDMS}$ for the PDMS layer and as $\sigma_{x,Pd\text{-}PDMS}$ and $\sigma_{y,Pd\text{-}PDMS}$ for the Pd/PDMS layer, respectively [22]. With increase in the annealing temperature, the value of $\Delta\sigma_x$ increases because the compressive stresses may mainly applied to X-axis in the PDMS layer and to Y-axis in the PDMS/Pd layer $\left(\Delta\sigma_x = \sigma_{x,PDMS} - \sigma_{x,Pd-PDMS}\right)$, as shown in Fig. 5(a). In case of a flat film, there is no preferred orientation for the wrinkles because the stress of the film has equi-biaxial state. When nanogaps are present, however, the stress in the film will be influenced by

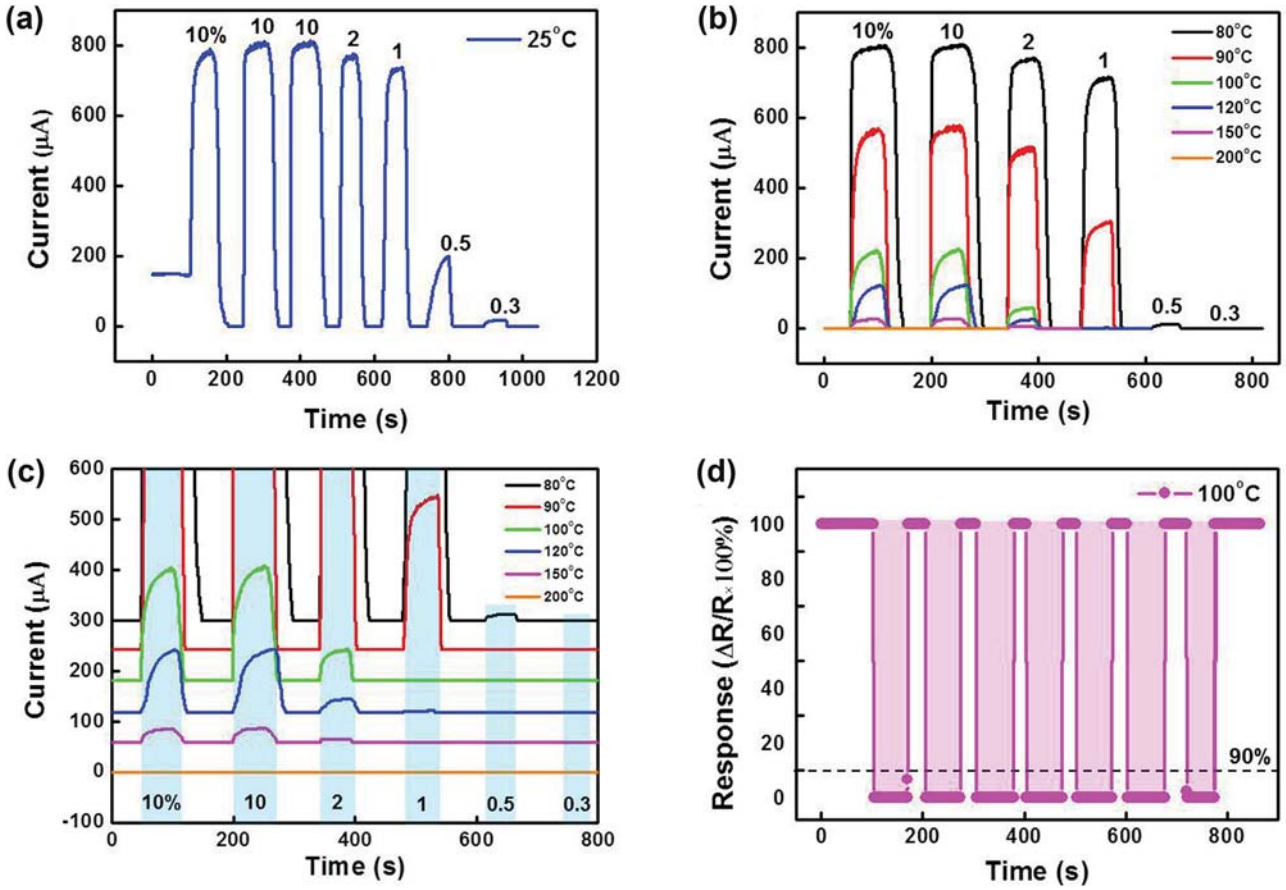

Fig. 4. (a) Real-time electrical responses of the Pd nanogap sensors at room temperature in N_2 and (b) its temperature dependent responses from 80 to 200 °C along with (c) the magnified base current responses. The curves are incrementally shifted upward by 60 μA for the clarity. (d) Sensor response versus time plot of the Pd nanogap sensors at 100 °C in 10% H_2. (The time interval is 1s).

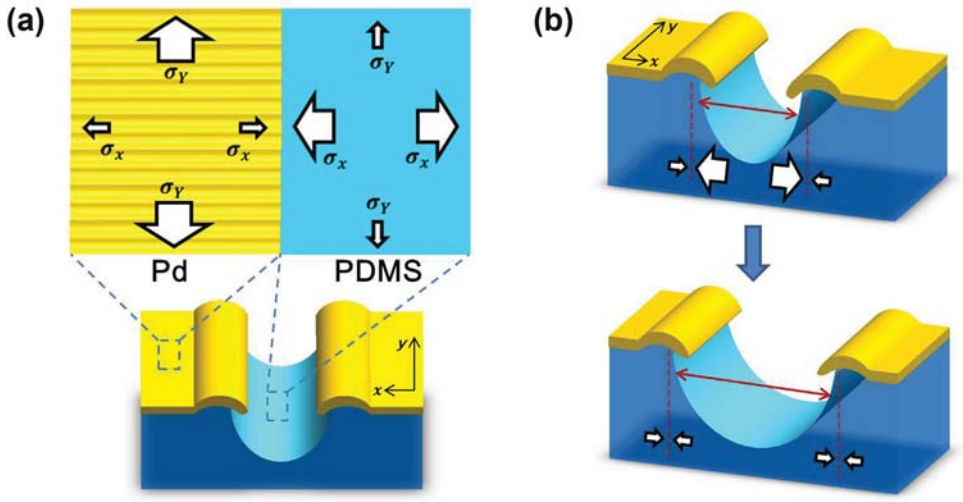

Fig. 5. (a) Schematic representation of the mechanism of Pd buckling on PDMS and the related compressive stresses in the X and Y axes along with the (b) nanogap broadening.

a strong orientation in the vicinity of the nanogaps ($\sigma_{x,PDMS}$ and $\sigma_{y,PDMS}$), with principal compressive stress direction ($\Delta\sigma_x$ and σ_y). Therefore, the sinusoidal wrinkles are aligned perpendicular to the nanogap direction [30]. In addition, the strain in the PDMS layer is much higher than the critical strain in the Pd/PDMS layer. Thus, the width of the Pd nanogap increased with the increase in the annealing temperature up to $\Delta\sigma_x = 0$ (Fig. 5(b)). The H_2 sensing performances were significantly affected by the width of the Pd nanogap.

Real time electrical response of Pd MOTIFE sensors, which annealed at various temperatures (90–150 °C) are measured with repeating cycles of H_2, respectively (Fig. 7). Each sensor showed similar saturated current level like Fig. 4(b) and consistent current response in identical H_2 concentration. Even though the perfor-

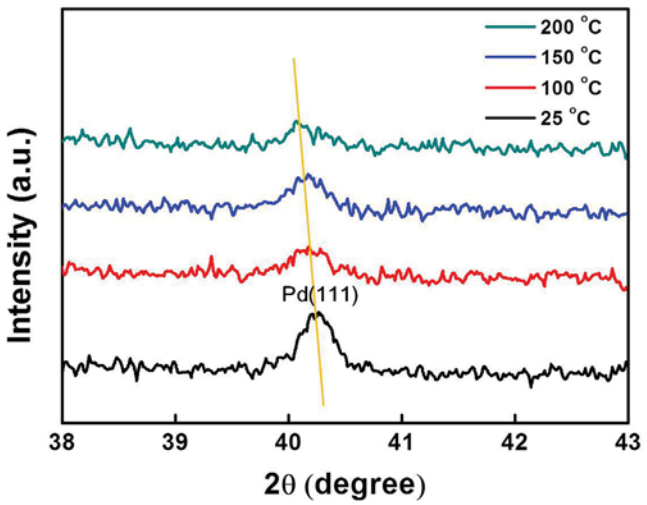

Fig. 6. The XRD patterns of the Pd nanogap sensors with different annealing temperature.

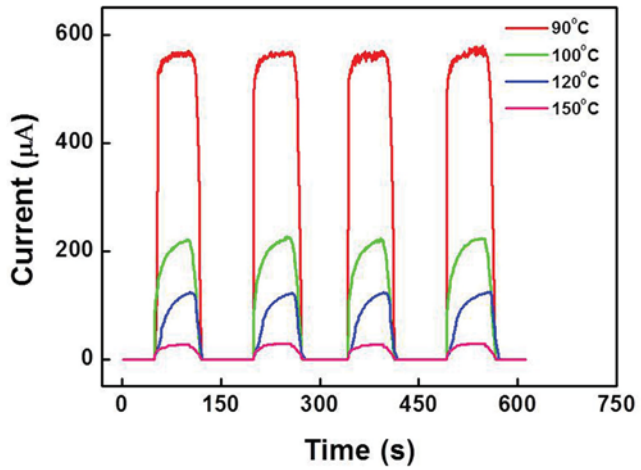

Fig. 7. Reproducibility tests of the real-time electrical responses of the annealed Pd nanogap sensors in 10% H_2.

mance of the sensor is debased due to thermal denaturalization of elastomer substrate, stable response was repeated without significant change of signal.

4. Conclusion

We investigated the influence of annealing temperature on the H_2 sensing performance of Pd based MOTIFE sensors. These sensors were fabricated on an elastomeric substrate by depositing Pd thin films. On the surface of the Pd/PDMS layer, nanocracks were initiated with intervals of about 15 μm by the application of mechanical stretching to up to 50% elongation, and converted to more stable nanogaps through exposure to H_2. During the annealing, the wrinkles were caused vertically against the nanogaps on the surface of the Pd/PDMS layer to release the stress resulting from a mismatch of thermal the expansion coefficients between the PDMS layer and the Pd film. With increase in the annealing temperature, the wrinkling wavelength decreased and the Pd nanogap width increased because of increases in the variations in the compressive stress and strain between PDMS and the Pd/PDMS layers. The enlarged Pd nanogap resulted in a decrease in the H_2 sensing performance. Nevertheless, the Pd-based MOTIFE sensor exhibited perfect on-off responses and fast response times (<1 s) when annealed at temperatures up to 100 °C.

Acknowledgments

This work is supported by the Priority Research Centers Program (2009-0093823) through the National Research Foundation of Korea (NRF) and "The Project of Conversion by the Past R&D Results" through the Ministry of Trade, Industry and Energy(MOTIE) and the Korea Institute for the Advancement of Technology(KIAT) (N0001532, 2015) and Korea Ministry of Environment as "Convergence Technology Program (2015001650001)".

Appendix A. Supplementary data

Supplementary data associated with this article can be found, in the online version, at http://dx.doi.org/10.1016/j.snb.2016.08.140.

References

[1] W.J. Buttner, M.B. Post, R. Burgess, C. Rivkin, An overview of hydrogen safety sensors and requirements, Int. J. Hydrogen Energy 36 (2011) 2462–2470.
[2] M. Momirlan, T.N. Veziroglu, The properties of hydrogen as fuel tomorrow in sustainable energy system for a cleaner planet, Int. J. Hydrogen Energy 30 (2005) 795–802.
[3] J.G. Firth, A. Jones, T.A. Jones, Principle of the detection of flammable atmospheres by catalytic devices, Combust. Flame 21 (1973) 303–311.
[4] L. Boon-Brett, J. Bousek, G. Black, P. Morretto, P. Castello, T. Hubert, U. Banach, Identifying performance gaps in hydrogen safety sensor technology for automotive and stationary applications, Int. J. Hydrogen Energy 35 (2010) 373–384.
[5] C. Wadell, S. Syrenova, C. Langhammer, Plasmonic hydrogen sensing with nanostructured metal hydrides, ACS Nano 8 (2014) 11925–11940.
[6] H. Gu, Z. Wang, Y. Hu, Hydrogen gas sensors based on semiconductor oxide nanostructures, Sensors 12 (2012) 5517–5550.
[7] A. Kaniyoor, R.I. Jafri, T. Arockiadoss, S. Ramaprabhu, Nanostructured Pt decorated graphene and multi walled carbon nanotube based room temperature hydrogen gas sensor, Nanoscale 1 (2009) 382–386.
[8] L. Al-Mashat, H.D. Tran, W. Wlodarski, R.B. Kaner, K. Kalantar-Zadeh, Conductometric hydrogen gas sensor based on polypyrrole nanofibers, IEEE Sens. J. 8 (2008) 365–370.
[9] F. Favier, E.C. Walter, M.P. Zach, T. Benter, R.M. Penner, Hydrogen sensors and switches from electrodeposited palladium mesowire arrays, Science 293 (2001) 2227–2231.
[10] Y. Im, C. Lee, R.P. Vasquez, M.A. Bangar, N.V. Myung, E.J. Menke, R.M. Penner, Investigation of a single Pd nanowire for use as a hydrogen sensor, Small 2 (2006) 356–358.
[11] Y. Sun, H.H. Wang, High-Performance, flexible hydrogen sensors that use carbon nanotubes decorated with palladium nanoparticles, Adv. Mater. 19 (2007) 2818–2823.
[12] S. Cherevko, N. Kulyk, J. Fu, C.-H. Chung, Hydrogen sensing performance of electrodeposited conoidal palladium nanowire and nanotube arrays, Sens. Actuators B 136 (2009) 388–391.
[13] J. van Lith, A. Lassesson, S.A. Brown, M. Schulze, J.G. Partridge, A. Ayesh, A hydrogen sensor based on tunneling between palladium clusters, Appl. Phys. Lett. 91 (2007) 181910.
[14] X.Q. Zeng, M.L. Latimer, Z.L. Xiao, S. Panuganti, U. Welp, W.K. Kwok, T. Xu, Hydrogen gas sensing with networks of ultrasmall palladium nanowires formed on filtration membranes, Nano Lett. 11 (2011) 262–268.
[15] J. Noh, H. Kim, B.S. Kim, E. Lee, H.H. Cho, W. Lee, High-performance vertical hydrogen sensors using Pd-coated rough Si nanowires, J. Mater. Chem. 21 (2011) 15935–15939.
[16] J. Lee, W. Shim, J. Noh, W. Lee, Design rules for nanogap-Based hydrogen gas sensors, ChemPhysChem 13 (2012) 1395–1403.
[17] J. Lee, W. Shim, E. Lee, J. Noh, W. Lee, Highly mobile palladium thin films on an elastomeric substrate: nanogap-based hydrogen gas sensors, Angew. Chem. Int. Ed. 50 (2011) 5301–5305.
[18] E. Lee, J. Lee, J. Noh, W. Kim, T. Lee, S. Maeng, W. Lee, Pd–Ni hydrogen sponge for highly sensitive nanogap-based hydrogen sensors, Int. J. Hydrogen Energy 37 (2012) 14702–14706.
[19] B. Jang, S. Cho, C. Park, H. Lee, M.J. Song, W. Lee, Palladium nanogap-based H_2 sensors on a patterned elastomeric substrate using nanoimprint lithography, Sens. Actuators B 221 (2015) 593–598.
[20] B. Jang, K.Y. Lee, J. Noh, W. Lee, Nanogap-based electrical hydrogen sensors fabricated from Pd-PMMA hybrid thin films, Sens. Actuators B 193 (2014) 530–535.
[21] J. Lee, J. Noh, S. Lee, B. Song, H. Jung, W. Kim, W. Lee, Cracked palladium films on an elastomeric substrate for use as hydrogen sensors, Int. J. Hydrogen Energy 37 (2012) 7934–7939.
[22] W.T.S. Huck, N. Bowden, P. Onck, T. Pardoen, J.W. Hutchinson, G.M. Whitesides, Ordering of spontaneously formed buckles on planar surfaces, Langmuir 16 (2000) 3497–3501.

[23] P. J. Yoo, H. H. Lee, Morphological Diagram for Metal/Polymer Bilayer Wrinkling: Influence of Thermomechanical Properties of Polymer Layer, Macromolecules, 38 (2820) 2820–2831.
[24] W.M. Choi, J. Song, D.Y. Khang, H. Jiang, Y.Y. Huang, J.A. Rogers, Biaxially stretchable "Wavy" silicon nanomembranes, Nano Lett. 7 (2007) 1655–1663.
[25] D.Y. Khang, J.A. Rogers, H.H. Lee, Mechanical buckling: mechanics, metrology, and stretchable electronics, Adv. Funct. Mater. 18 (2008) 1–11.
[26] N. Bowden, W.T.S. Huck, K.E. Paul, G.M. Whitesides, The controlled formation of ordered, sinusoidal structures by plasma oxidation of an elastomeric polymer, Appl. Phys. Lett. 75 (1999) 2557–2559.
[27] I.D. Johnston, D.K. McCluskey, C.K.L. Tan, M.C. Tracey, Mechanical characterization of bulk Sylgard 184 for microfluidics and microengineering, J. Micromech. Microeng. 24 (2014) 035017.
[28] B. Kim, M. Park, Y.S. Kim, U. Jeong, Thermal expansion and contraction of an elastomer stamp causes position-dependent polymer patterns in capillary force lithography, ACS Appl. Mater. Interfaces 3 (2011) 4695–4702.
[29] F. Schneider, T. Fellner, J. Wilde, U. Wallrabe, Mechanical properties of silicones for MEMS, J. Micromech. Microeng. 18 (2008) 065008.
[30] N. Bowden, S. Brittain, A.G. Evans, J.W. Hutchinson, G.M. Whitesides, Spontaneus formation of ordered structures in thin films of metals supported on an elastomeric polymer, Nature 393 (1998) 146–149.

Biographies

Byungjin Jang was born in 1987 in Seoul, Republic of Korea. He received a BS degree in Material Science and Engineering at Yonsei University in 2012. He is currently studying MOTIFE sensors using Pd as a step toward his Ph.D. degree in hydrogen sensor devices at Yonsei University.

Wonkyung Kim was born in 1976 in Mokpo, Republic of Korea. He received a B.E. in Material Science and Engineering at Yonsei University in 2007. He has been a High school teacher since 2002. He is currently studying MOTIFE sensors using Pd as a step toward his Ph.D. degree in hydrogen sensor devices at Yonsei University.

Min-Jung Song received her Ph.D. in chemical engineering from Korea University (2007). Now she is working as an associate professor at Kyonggi University. Her research interests are focused on the bio-sensors, gas sensors, electroanalysis, and bio-MEMS.

Wooyoung Lee is a professor of Department of Materials Science and Engineering, the chairman of Yonsei Institute of Convergence Technology and the Head of Institute of Nanoscience and Nanotechnology at Yonsei University in Korea. He received a BS degree in metallurgical engineering in 1986, a MS degree in metallurgical engineering from the Yonsei University in 1988. He received a Ph.D. degree in physics from University of Cambridge, England in 2000. He is also the director in Korea-Israel Industrial R&D Foundation and the advisor in National Assembly Research Service. In recent years, his research interests have centered on thermoelectric devices, spintronics, hydrogen sensors and hydrogen storage materials. He has received a number of awards in nano-related research areas and a Service Merit Medal (2008) from the Korean Governments due to contribution on the development of intellectual properties. He has authored and co-authored over 150 publications, and has edited a few of special books on nano-structured materials and devices.